Title
Pion Correlations for 1.2 A GeV Lanthanum on Lanthanum

Journal
Physical Review C, 47(2)

Authors
Christie, W.B.
Olson, D.L.
Tull, C.E.
et al.

Publication Date
1992-06-01

LBL-32437
UC-414
Preprint

Lawrence Berkeley Laboratory
UNIVERSITY OF CALIFORNIA

Submitted to Physical Review C

Pion Correlations for 1.2 A GeV Lanthanum on Lanthanum

W.B. Christie, D.L. Olson, C.E. Tull, F.P. Brady, G.P. Grim, J.H. Osborne, M.L. Partlan, J.L. Romero, J. Chang, S.Y. Fung, J. Kang, S. Zhang, D. Keane, and Y. Dardenne

June 1992

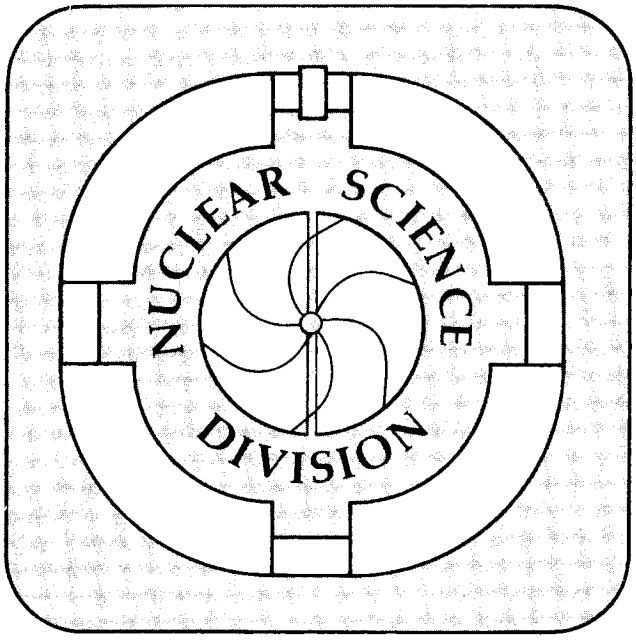

Prepared for the U.S. Department of Energy under Contract Number DE-AC03-76SF00098

DISCLAIMER

LBL-32437
UC-414

Submitted to Physical Review C

Pion Correlations for 1.2 A GeV Lanthanum on Lanthanum

W.B.Christie and D.L.Olson
Lawrence Berkeley Laboratory, Berkeley, California, 94720

C.E. Tull
Louisiana State University, Baton Rouge, Louisiana, 70803

F.P.Brady, G.P. Grim, J.H. Osborne, M.L. Partlan, J.L.Romero
University of California, Davis, California 95616

J. Chang, S.Y.Fung, J. Kang, S. Zhang
University of California, Riverside, California 92521

D. Keane
Kent State University, Kent, Ohio 44242

Yves Dardenne
Michigan State University, East Lansing, Michigan, 48823

June 1992

This work was supported by the Director, Office of Energy Research, Division of Nuclear Physics of the Office of High Energy and Nuclear Physics of the U.S. Department of Energy under Contract DE-AC03-76SF00098

Pion correlations for 1.2·A GeV Lanthanum on Lanthanum

W.B.Christie, D.L.Olson
Lawrence Berkeley Laboratory, Berkeley California 94720

C.E.Tull
Louisiana State University, Baton Rouge Louisiana, 70803

F.P.Brady, G.P.Grim, J.H.Osborne, M.L.Partlan, J.L.Romero
University of California, Davis California 95616

J.Chang, S.Y.Fung, J.Kang, S.Zhang
University of California, Riverside California 92521

D. Keane
Kent State University, Kent Ohio 44242

Yves Dardenne
Michigan State University, East Lansing Michigan, 48823

(Received:

Results are presented for pion interferometry measurements of 1.2·A GeV La + La at the Lawrence Berkeley Laboratory Heavy Ion Spectrometer System (HISS). The experiment's acceptance is at forward angles in the center of mass system. The fit parameters R, τ, λ, $R_\perp$, and $R_\parallel$ are presented. The correlation between the extracted size of the pion source and the centrality of the collision is investigated as well as the dependence of the source size on the mean momentum of the pion pairs. We conclude that the fitted radius parameters scale with mass for symmetric systems. We observe a clear dependence of the fitted size of the pion source on the mean momentum of the pion pairs. Comparisons are made with previous results.

PACS number 25.75.+r

Introduction

Reported here are the results from an extension of experiment E684H. Experiment E684H, reported earlier[1], and the extension were performed at Lawrence Berkeley Laboratory, using the Heavy Ion Spectrometer System (HISS). Due to the similarity of the experimental setup, detectors, and analysis used, we will avoid reproducing most of these details in this report.

A simple geometric model is usually used when describing high energy nucleus - nucleus collisions. In this model,[2 - 4]commonly referred to as abrasion - ablation or participant - spectator, when the two nuclei collide the overlap regions of the two nuclei interact with one another, forming a hot, dense, interaction region, while the remaining parts of the projectile and target nuclei are left largely unaffected aside from some excitation energy. It is this interaction region which we wish to study.

To extract some measure of the volume of the interaction region, and, if one knows the number of participants, the density, one may use the correlations of identical particles[5 - 13]. The application of this technique, commonly referred to as the Goldhaber, Goldhaber, Lee, and Pais[13](GGLP) or Hanbury-Brown, Twiss[5] (HBT) technique, and results for 1.2·A GeV lanthanum on lanthanum is the subject of this report.

Intensity Interferometry

The derivation of the pion correlation function can be found in many papers.[9,10,14] For two identical bosons the correlation function is given by:

$$C_2(q,q_0) \equiv 1 + |\rho(q,q_0)|^2 \qquad (1)$$

where $q = | p_1 - p_2 |$ is the relative three momentum, $q_0 = | E_1 - E_2 |$, and $\rho(q,q_0)$ is the Fourier transform of the pion emitting source distribution. To continue, one must make some assumption for the form of this distribution. Following the work of Yano and Koonin[10] we have chosen to use their Gaussian formulation for the spatial and temporal distribution. This distribution is parameterized as:

$$\rho(r_\perp, r_\parallel, t) = \alpha\, e^{(-r_\perp^2/R_\perp^2 - r_\parallel^2/R_\parallel^2 - t^2/\tau^2)} \qquad (2)$$

or with the assumption that $R_\perp = R_\parallel$, as:

$$\rho(r,t) = \alpha\, e^{(-r^2/R^2 - t^2/\tau^2)}. \qquad (3)$$

$R_\perp$ (denoted R_T in Figs.) and $R_\parallel$ above refer to the directions transverse to, and parallel to, the beam, respectively. α is merely a normalization constant. Using this form for $\rho(r,t)$ leads to:

$$C_2(q,q_0) = 1 + e^{(-q^2R^2/2 - q_0^2\tau^2/2)} \quad (4)$$

Notice that the expression for C_2 approaches the value of two as q and q_0 both go to zero, as one would expect for identical bosons. To get a better fit to the data it was first suggested by Deutschmann *et al.*[15] that one put another fit parameter in front of the exponent in the function above. This parameter, typically given the symbol lambda, is usually referred to as the chaoticity or coherence parameter. It allows for a decrease in the magnitude of the two pion enhancement due to partial coherence of the emitted pions as well as other physical processes[16] acting on the pions. Our final two - pion correlation function is thus:

$$C_2(q,q_0) = 1 + \lambda e^{(-q^2R^2/2 - q_0^2\tau^2/2)} \text{ or} \quad (5)$$

$$C_2(q_\perp,q_\parallel,q_0) = 1 + \lambda e^{(-q_\perp^2R_\perp^2/2 - q_\parallel^2R_\parallel^2/2 - q_0^2\tau^2/2)} \quad (6)$$

the choice of form depending on whether one assumes the source is spherical.

The theoretical two pion correlation function is defined as the normalized ratio of the inclusive two pion cross section to the product of the single pion cross sections.[11] While this gives an exact definition of the correlation function it is not the function which is actually fit to the data. Experimentally one extracts a quantity which is the pion pair distribution as a function of q and q_0, or some other parameters related to the pions separation in phase space, for pairs in which one expects to see the enhancement in the distribution due to the Bose statistics, and divides this by the same distribution for pion pairs in which one expects most effects *except* those due to the Bose statistics. We will refer to those pairs in which one expects the correlation to manifest itself as correlated pairs, and those in which one does not expect the effect as uncorrelated pairs.

The technique which was employed in this analysis to form the uncorrelated pairs is most commonly known as *event mixing*. With this scheme one forms the correlated pairs by using pions from within a given event. The uncorrelated background pairs are formed by mixing pions from different events. It is clear that with this method most of the hardware and software acceptances are automatically taken into account. When using this method one must take great care to use as close to the same type of events as possible in forming the correlated and uncorrelated pairs. In this analysis care has been taken to use exactly the same set of pions in both the correlated and uncorrelated pion pairs.

Experimental Setup

This experiment was performed using the Heavy Ion Spectrometer System[17] (HISS) which is located at the Lawrence Berkeley Laboratory Bevalac. The HISS configuration used for this experiment was almost identical to that used in our previous pion experiment and is shown in Fig. 1. The event centrality selection is accomplished by triggering on events with low analog signals in the V_4 Cerenkov radiator. Details on the various detectors can be found in Ref. 1.

The acceptance for the experiment, evaluated in the nucleon - nucleon c.m. frame, is shown in Figs. 2, 3, and 4. The coordinates are defined such that Px is the component of momentum in the bending plane of the HISS dipole, Py is the vertical or out of bending plane component, and Pz is the component in the direction of the beam, i.e. the longitudinal component.

Fig. 2 shows a histogram of the inclusive momentum distribution for a random subset of the negative pions which are accepted into the HBT analysis (i.e. come from events with two or more π^-). Fig. 3a shows the acceptance in P_x versus P_z. Fig. 3b shows the acceptance in P_y versus the magnitude of the momentum. Fig. 3c shows the inclusive distribution of θ_x for a random subset of the pions used in the correlation analysis. They come from a distribution of angles with a mean of about 6° and a σ of about 32°.

Fig. 4 shows the acceptance for the pion pairs, in particular the distribution for the relative momentum of the pairs (q) and the relative energy of the pion pairs(q_0). The increasing contour labels represent increasing numbers of counts. Notice that only half of the q - q_0 plane is populated. This is due to a constraint imposed by relativistic kinematics.

The momentum resolution of interest for the pions used in the correlation analysis presented here is about 2.5% ($\Delta p/p$) in the nucleon - nucleon c.m. frame[1]. This includes the multiple Coulomb scattering of the pions in the target and all material downstream to the end of the drift chambers as well as the position resolution of the drift chambers. Not included is the position resolution of the beam on the target which cancels in first order when one uses the relative momenta of the pions.

Triggers and Data Set

We used a single trigger to collect all the data used in this analysis. We cycled, run to run, between the Lanthanum target and an empty target to minimize any time dependent systematics. The trigger used was: $S_1 \cdot \overline{V_1} \cdot S_2 \cdot \overline{V_2} \cdot \overline{V_4}$. The soft collimator (scintillator with a hole) - scintillator arrangements, $\overline{V_1} \cdot S_1$ and $\overline{V_2} \cdot S_2$,

identify (roughly) the upstream beam nuclei accepted by the trigger. V_4 is a Cerenkov radiator, placed downstream of the HISS dipole, which is used to select the centrality of the events accepted by the trigger.

The lanthanum target was 0.801 g/cm^2 thick. The total number of events collected with the Lanthanum target was approximately 2.5 million. The cross section for satisfying the trigger, corrected for deadtime and target out, was 1.80 barn. Comparing to the calculated geometric cross section for Lanthanum on Lanthanum:

$$\sigma_{geo} = \pi r_0^2 (A_b^{\frac{1}{3}} + A_t^{\frac{1}{3}})^2 \qquad (7)$$

one finds that the trigger corresponds to about 37% of σ_{geo}. In the equation above, r_0 = 1.2 fm and A_b and A_t are the number of nucleons in the beam and target nuclei.

Systematic Corrections

There are three systematic effects which we've corrected for in the analysis. In all cases the systematic corrections are applied by weighting the uncorrelated π^- pairs.

The first correction is for the detection efficiency of the Drift Chamber (DC), due to both hardware and software, for finding close tracks[1]. The effect of this efficiency correction on the HBT fits was very small (see Table 1 where we have included the results of the HBT fits with and without the DC efficiency correction applied).

The second correction is for the effect due to the mutual Coulomb repulsion between the pions in the correlated pairs. For the repulsive Coulomb interaction between the two π^- in a pair this penetration factor is the Gamow factor [11] :

$$G(\eta) = \frac{2\pi\eta}{e^{2\pi\eta}-1} \qquad \text{where } \eta = \frac{m_\pi \alpha}{\sqrt{q_0^2 - q^2}} \qquad (7)$$

The Gamow correction factor is applied to the uncorrelated pion pairs before the HBT function is fit. The Gamow correction has a substantial effect on the λ parameter and a relatively small effect on the radius parameter (see Table 1). The magnitude of the correction to λ is very similar to some earlier results[1,18].

The third correction is for residual correlations in the uncorrelated pairs. This correction technique was first derived and applied by Zajc[14] in his analysis of a pion interferometry experiment using the Janus spectrometer at the BEVALAC. Its purpose is to correct for the distortion in the single pion inclusive spectra due to the

Bose Einstein correlations. The correction is performed with an iterative procedure in which one weights the uncorrelated pion pairs[1].

Results

We have tabulated the fits to the two forms of the correlation function given in equations 5 and 6. All the fits were performed in the nucleon - nucleon center of mass frame.

The results of the fits on the full data set are shown in Table 1 with the following combinations of systematic corrections applied: no corrections, just the DC efficiency correction, both the DC efficiency and the Gamow corrections, and the DC efficiency, Gamow, and correction for Background correlations all applied. Where calculated, the one σ errors in the fit are given for the parameters. Also listed in the tables are the χ^2 and the number of independent degrees of freedom (NDF) for the fit. Using these two quantities we have calculated what is known[19] as the *upper - tail area function* using the first approximation to χ^2. This upper - tail area function (UTAF) gives the probability of getting a value for χ^2 greater (or less) than that measured. Its value is the percentage of the area of the χ^2 distribution between the value for $\chi 2$ which one obtains from the fit to the nearest end of the distribution. For a perfect fit this function reaches its maximum value of one half. For all fits the range of the independent variables (i.e. q, q_0, $q_\perp$, $q_\parallel$) was from zero to four hundred (MeV/c, MeV).

Also given are the number of correlated and uncorrelated π^- pairs used in each of the fits. The variation in the number of π^- pairs used in the fits is due to the different numbers of matrix bins into which the pairs are placed (i.e. $C(q, q_0)$ or $C(q_\perp, q_\parallel, q_0)$) and the requirement that all bins used in the fits contain at least five correlated pairs.

Full Data Set

The trigger selected $\approx$ 37% of the geometric cross section for the Lanthanum on Lanthanum system. Approximately 3% of the events accepted by the trigger contained two π^- which were passed for further analysis. We collected approximately 2.5 million raw events and ended up with $\approx$ 94 thousand correlated pion pairs which passed all the quality cuts. Bin widths of 10 MeV (MeV/c) were used in the first set of fits in the table and widths of 20 were used in the second set of fits ($C_2(q_\perp, q_\parallel, q_0)$). The results are listed in Table 1.

Fig. 5a shows the experimental correlation data (i.e. the distribution as a function of q and q_0 of the correlated π^- pairs divided by the same distribution for the uncorrelated pairs). The fitted theoretical correlation function is shown in plot 5b. The

data and fit shown correspond to the first set of fit parameters (R, τ, and λ) in Table 1, with the DC efficiency and Gamow corrections applied. Notice the expected enhancement in the ratio of correlated to uncorrelated π^- pairs in the low q - q_0 region. Bin widths shown are 10 MeV/c by 10 MeV.

As the extracted lifetime parameter is zero for the fit to R, τ, and λ shown, and because historically others have shown correlation results in this manner, Figs. 6a and b show the data and the fit, without and with the DC efficiency and Gamow corrections applied, projected onto the q axis. The error bars shown are just the statistical errors. The solid lines are the fitted HBT function.

When one plots the error contours, the correlation between the various fit parameters can be examined. Shown in Fig. 7 are the error contours for the parameters R, τ, and λ. The DC efficiency, Gamow, and correction for background correlations are applied. The contours shown correspond to the one and two standard deviation errors. The positive correlation shown between the chaoticity parameter λ and the radius parameter R is as one would expect: an increase in R can be compensated for by an increase in λ, and has been seen previously. The lack of an appreciable correlation between the radius and lifetime parameters (i.e. error contours are parallel to the axes) is a consequence of the large acceptance of the experimental setup, which has the desirable effect of uncoupling the determination of the two parameters.

Fig. 8 shows the error contours for the spatial parameters $R_\perp$ and $R_\parallel$ versus those for the lifetime parameter τ. Notice the correlation between the parameters $R_\parallel$ and τ and the lack of a correlation between the parameters $R_\perp$ and τ. This is to be expected due to the coupling of the relative energy and the relative parallel momentum for pions close to zero degrees.

It has been suggested by Beavis *et al*[20] and by Pratt[21] that one may be able to extract information about the evolution of the pion emitting source by performing the HBT analysis as a function of the mean momentum of the pion pairs in the cm frame. Pratt's model incorporates the radial expansion aspects of the hot participant region, as theorized by Siemens and Rasmussen[22], to see how the pion interferometry analysis is affected. What he finds is that the radius parameter R decreases monotonically as a function of K ($\mathbf{K} = \mathbf{p}_1 + \mathbf{p}_2$), and that R decreases faster as the ratio of the energy in collective expansion to thermal energy is increased. The physical explanation Pratt gives for this effect is that the faster pion pairs are most likely emitted from a point on the expanding shell which is in the direction of K, and therefore appear to come from a smaller effective source. He also points out that another

possible explanation could be that as the pion- nucleon cross section falls off rapidly for relative energies above 140 MeV due to the Delta resonance, the faster pions may have a larger mean free path and hence a higher probability of escaping during the early stages of the collision while the source is small.

The distribution of the mean momentum $((|P_1|+|P_2|)/2)$ for the π^- pairs is shown in Fig. 9. The π^- pairs in the low and high regions of the distribution, with mean momentum below 170 MeV/c and above 230 MeV/c, were fit and the results are shown in Table 2. Fig. 10 shows the one sigma error contours for the fit parameters R, τ, and λ from the fits to the two regions. In Fig. 11 we've ploted the one sigma error contours for the fit parameters $R_\perp$ and $R_\parallel$. Notice the clear reduction in the magnitude of the radius parameters R and $R_\perp$ for the higher mean momentum π^- pairs.

The fits shown in Table 2 and the plots shown in Figs. 10 and 11 are consistent with the trend which Beavis and Pratt predict. The decrease in radius is similar to results obtained for 1.5·A GeV Ar on KCl data taken at the LBL streamer chamber by D. Beavis *et al*[19]. The magnitude of the effect we see is smaller than observed in their data, although one must note that the range of the mean pion momentum in our data is also smaller. As pointed out in their paper, the decrease of the extracted radius as a function of the pion momentum is consistent with a pion fireball model in which the temperature decreases as the source expands. In a later paper by the same group for 1.8·A GeV Ar on Pb this effect of a decreasing radius as one increases the mean value of the pion pair's momentum was also observed[23].

To investigate whether we could extract a correlation between the centrality of the collision and the fitted radius parameters we placed cuts on the ADC spectrum of the TOF wall which views the projectile spectator fragments. Shown in Fig. 12 is the ADC spectrum for the TOF wall. HBT fits were performed on the group of events which had ADC values equal to or less than 100 and the group of events which had ADC values greater than or equal to 400. These bounds are indicated by the vertical dashed lines in Fig. 12. The results of these cuts are listed in Table 3. Fig. 13 shows the one sigma error contours for the parameters $R_\perp$ and $R_\parallel$ resulting from the two fits. The DC efficiency and Gamow corrections were applied in the fits shown. The fits show the dependence which one would expect to observe if the cut was indeed sensitive to the impact parameter and the fitted HBT radius parameters are proportional to the geometric size of the source. One expects the transverse ($R_\perp$) radius to vary almost linearly with b, while the expected dependence of $R_\parallel$ on the impact parameter is less obvious.

Discussion

We believe that the results reported here, along with our previous results[1] for Ar on KCl, demonstrate for the first time, with unambiguous statistics and the same experimental apparatus and analysis, that there is a direct correlation between the mass of a symmetric heavy ion system and the fitted radius parameters. This is shown graphically in Fig. 14.

In both of our experiments we had "central" collision triggers, the cross sections for the triggers being about 26% and 37% of the geometric cross sections for Ar on KCl and La on La respectively. One expects that the mean impact parameters for the events which are used in the analyses are further reduced by the requirement that two or more negative pions are detected in the events; given the relatively low rate of pion production at this beam energy and the limited detector acceptance, this requirement is equivalent to demanding increased centrality for the accepted events. We infer that the fitted radius parameters give spatial information for the nucleus-nucleus interaction region. Consistent with this conclusion are the changes in the fitted radii we've observed when we've cut our data on distributions which we believe are proportional to the centrality of the collisions.

In a recent report on a compilation of the pion interferometry results from the Janus spectrometer[24] the authors concluded that there was no apparent scaling of the radius parameters with the mass of the colliding system. This clearly disagrees with our results.

The results of the fits for the high and low portions of the pion pair mean momentum distribution show a clear reduction in the fitted radius parameters R and $R_\perp$ for the high mean momentum pairs relative to the low mean momentum pairs. This is a three sigma effect for the single radius fit parameter R and a 2.3 sigma effect for $R_\perp$. This effect on the fit parameter R has been reported earlier by Beavis *et al*[20] , for 1.5 GeV·A Ar on KCl (~ 2 σ effect), and 1.8 GeV·A Ar on Pb[23] (~ 3 σ effect).We observed this same trend in our previous Ar on KCl data but the results were only suggestive. Chacon *et al*[25]looked for and did not observe this effect in their Nb on Nb data.

We conclude that there is a dependence of the fitted radius parameters on the mean momentum of the pion pairs. The dependence is consistent with the model where the high mean momentum pions escape quickly while the interaction region is hot and dense, while the lower momentum pions escape later from a cooler, expanding

source, and thus may provide a method to study the temporal evolution of the pion source.

Acknowledgements

This work was supported by NSF grant PHY87-22008, DOE grant DE-FG03-86ER40271, and by the Director of Energy Research, Division of Nuclear Physics of the Office of High Energy and Nuclear Physics of the U.S. Department of Energy under contract DE-AC03-76SF00098.

[1]W.B.Christie et al. Phys Rev. C. (in press).
W.B.Christie, Ph.D. Thesis(1990) University of California, Davis, LBL rep. #28986
[2] J. Hufner, K. Schafer, B. Schurmann, Phys. Rev. C **12**, 1888 (1975).
[3] D.J. Morrissey, W.R. Marsh, R.J. Otto, W. Loveland, G.T. Seaborg, Phys. Rev. C **18**, 1267 (1978).
[4] L.F. Oliveira, R. Donangelo, J.O. Rasmussen, Phys. Rev. C **19**, 826 (1979).
[5]R. Hanbury - Brown and Twiss, Nature **178** 1046 (1956).
[6] E.V. Shuryak, Phys. Lett. **44**B 387 (1973).
[7] G.I. Kopylov and M.I. Podgoretskii, Sov. J. Nuc. Phys. **18** 336 (1974).
[8] G. Cocconi, Phys. Lett. **49**B 459 (1974).
[9] S.E. Koonin, Physics Lett. **70**B 43 (1977).
[10] F.B. Yano and S.E. Koonin, Phys. Lett. **78**B 556 (1978).
[11]M. Gyulassy, S.K. Kauffman, L.W. Wilson, Phys. Rev. C **20** 2267 (1979).
[12]W.J. Knox, Phys. Rev. D **10** 65 (1974).
[13]G. Goldhaber, S. Goldhaber, W. Lee, A. Pais, Phys. Rev. **120** 300 (1960).
[14] W.A. Zajc, Ph.D. Thesis (1982) LBL report #14864.
W.A. Zajc *et al*, Phys. Rev. C **29** 2173 (1984).
W.A. Zajc, Nevis Lab report #1384, Columbia University.
[15] M. Deutchmann *et al.*, Cern/EP/Phys 78 - 1 (1978).
[16] M. Gyulassy, Phys. Rev. Lett. **48** 454 (1982).
[17]J. Engelage *et al*, Nucl. Instr. and Meth. A277 431 (1989).
[18] D. Beavis, S.Y. Chu, S.Y. Fung, W. Gorn, D. Keane, R. Poe, G. VanDalen, M. Vient, Phys. Rev. C **28**, 2561 (1983).
[19] Stuart L. Wilson, Data Analysis for Scientists and Engineers, John Wiley & Sons, Inc.
[20] D. Beavis, S.Y. Fung, W. Gorn, A. Huie, D. Keane, J.J. Lu, R. Poe, B. Shen, G. VanDalen, Phys. Rev. C **27**, 910 (1983).
[21] S. Pratt, Phys. Rev. Lett. **53**, 1219 (1984).
[22] P.J. Siemens and J.O. Rasmussen, Phys. Rev. Lett. **42**, 880 (1979).
[23] Y.M. Liu, D. Beavis, S.Y. Chu, S.Y. Fung, D. Keane, G. VanDalen, M. Vient, Phys. Rev. C **34**, (1986).
[24] H.Bossy et al, LBL report #31629 (1991).
[25] A.D.Chacon et al, Phys. Rev. C **43**, 2670 (1991).

Table 1 Results for 1.2 ·A GeV Lanthanum on Lanthanum

Systematic	DC efficiency		X	X	X
Corrections	Gamow			X	X
Applied	Background				X
R (fm)		6.39	6.35	6.34 ± 0.25	5.97 ± 0.24
τ (fm/c)		0.12	2.45	0.00 + 2.0	0.00 + 2.2
λ		0.53	0.56	0.79 ± 0.05	0.78 ± 0.06
$\frac{\chi 2}{NDF}$		$\frac{741.8}{661}$	$\frac{736.6}{661}$	$\frac{752.4}{661}$	$\frac{760.8}{661}$
UTAF		0.0010	0.0020	0.0003	$8.4 * 10^{-5}$
94,812 Correlated π^- pairs,		1,461,900 Uncorrelated π^- pairs.			
$R_\perp$ (fm)		6.13	6.10	6.29	5.91 ± 0.20
$R_\parallel$ (fm)		5.48	5.48	5.57	5.15 ± 0.35
τ (fm/c)		3.75	4.38	3.10	$3.43 \pm {}^{1.0}_{1.2}$
λ		0.50	0.53	0.77	0.77 ± 0.05
$\frac{\chi 2}{NDF}$		$\frac{1760.8}{1669}$	$\frac{1737.2}{1669}$	$\frac{1743.7}{1669}$	$\frac{1742.2}{1669}$
UTAF		0.013	0.048	0.034	0.037
93,036 Correlated π^- pairs,		1,421,700	Uncorrelated π^- pairs.		

Table 2 Results as a function of the mean momentum of the pion pairs.

Mean momentum for pion pairs	≦170 (MeV/c)	≧230 (MeV/c)
R (fm)	6.28 ± 0.40	4.30 ± 0.50
τ (fm/c)	$2.86 \pm {}^{2.0}_{2.86}$	$0.0 + 2.0$
λ	0.76 ± 0.08	0.63 ± 0.13
$\frac{\chi 2}{NDF}$	$\frac{223.8}{221}$	$\frac{619.6}{587}$
UTAF	0.41	0.09
Correlated π^- pairs	31,591	24,827
$R_\perp$ (fm)	6.23 ± 0.40	4.73 ± 0.50
$R_\parallel$ (fm)	5.20 ± 0.60	$4.53 \pm {}^{1.1}_{1.9}$
τ (fm/c)	$4.0 \pm {}^{1.3}_{1.9}$	$1.1 \pm {}^{2.8}_{1.1}$
λ	0.74 ± 0.07	0.68 ± 0.14
$\frac{\chi 2}{NDF}$	$\frac{395.9}{376}$	$\frac{1125.7}{1141}$
UTAF	0.15	0.33
Correlated π^- pairs	31,319	23,273

Table 3 Results as a function of $\sqrt{\text{BW ADC hi*lo.}}$

Mean momentum for pion pairs	≤100 (MeV/c)	≥ 400 (MeV/c)
R (fm)	6.62 ± 0.40	5.05 ± 0.50
τ (fm/c)	$0.0 + 3.2$	$1.5 \pm^{2.6}_{1.5}$
λ	0.83 ± 0.09	0.62 ± 0.10
$\frac{\chi 2}{NDF}$	$\frac{608.3}{618}$	$\frac{437.1}{406}$
UTAF	0.36	0.06
Correlated π^- pairs	44,916	13,447
$R_\perp$ (fm)	6.57 ± 0.40	5.17 ± 0.50
$R_\parallel$ (fm)	6.68 ± 0.60	6.18 ± 0.85
τ (fm/c)	$2.7 \pm^{2.1}_{2.7}$	0.0 ± 4.4
λ	0.81 ± 0.08	0.70 ± 0.09
$\frac{\chi 2}{NDF}$	$\frac{1041.4}{1133}$	$\frac{450.6}{466}$
UTAF	0.003	0.24
Correlated π^- pairs	42,202	11,564

Figure Captions

Figure 1. Experimental setup. Hiss B field is into the page with a magnitude of 7kG. Beam nuclei and projectile fragments mean trajectories are represented by the dashed line.

Figure 2. Inclusive momentum distribution for a random subset of the π^-, evaluated in the nucleon - nucleon c.m. frame, for events with two or more π^-.

Figure 3. Crosshatched regions in figures 3a and 3b show the acceptance for π^-. X is in bending plane of HISS dipole, Y is vertical, and Z is along beam direction. The inclusive θ_x distribution shown in figure 3c has a mean of 6.6° and $\sigma \approx 32°$.

Figure 4. Acceptance for correlated π^- pairs. q and q_0 are the relative momentum and energy, respectively, for the pairs. Increasing contour labels represent increasing numbers of counts.

Figure 5. $C(q,q_0)$ vs q and q_0. Plot 5a shows the experimental correlation data and plot 5b shows the fit. The DC efficiency and Gamow corrections are applied.

Figure 6. The correlation function projected onto the q axis. Plot a is with no corrections. Plot b is with Drift Chamber efficiency and Gamow corrections. Uncertainties shown are statistical.

Figure 7. One and two sigma error contours for standard R, τ, λ fit. Drift Chamber efficiency, Gamow, and correction for background correlations are applied.

Figure 8. One and two sigma error contours for $R_\parallel$ vs τ and R_T vs τ. Notice the coupling between the parameters $R_\parallel$ and τ and the absence of any coupling (error contours parallel to axes) between R_T and τ. Drift Chamber efficiency, Gamow, and background correlation corrections are applied.

Figure 9. Distribution for the mean momentum $((|P_1|+|P_2|)/2)$ for a random subset of the correlated π^- pairs, evaluated in the nucleon-nucleon c.m. frame. Fits were performed separately on those pairs with mean momentum below the line at 170 MeV/c (mean = 146 MeV/c, σ = 15 MeV/c) and those above the line at 230 MeV/c (mean = 289 MeV/c, σ = 58 MeV/c).

Figure 10. One sigma error contours for R, τ, and λ fit parameters for the fits to the high and low portions of the mean pion pair momentum distribution shown in figure 9. Fits were done with DC efficiency and Gamow corrections applied. Fit values are listed in table 2.

Figure 11. One sigma error contours for R_T vs $R_\parallel$ fit parameters for the fits to the high and low portions of the mean pion pair momentum distribution shown in figure 9. Fits were done with DC efficiency and Gamow corrections applied. Fit values are listed in table 2.

Figure 12. Distribution of $\sqrt{\text{ADC hi*lo}}$ for the slat in the Fragment wall with the largest value of $\sqrt{\text{ADC hi*lo}}$ in the event. Fits were done separately to those events which were to the left of the line at 100 and to the right of the line at 400.

Figure 13. One sigma error contours for R_T vs $R_\parallel$ fit parameters for the fits to the high and low portions of the $\sqrt{\text{ADC hi*lo}}$ distribution shown in figure 12. Fits were done with DC efficiency and Gamow corrections applied. Fit values are listed in table 3.

Figure 14. Summary plot of R_T vs $R_\parallel$ for three systems studied in our previous experiment as well as the La on La system reported here. One sigma error contours are shown. Dashed line is for reference and represents $R_T = R_\parallel$. DC efficiency, Gamow, and background correlation corrections are applied for all four fits shown.

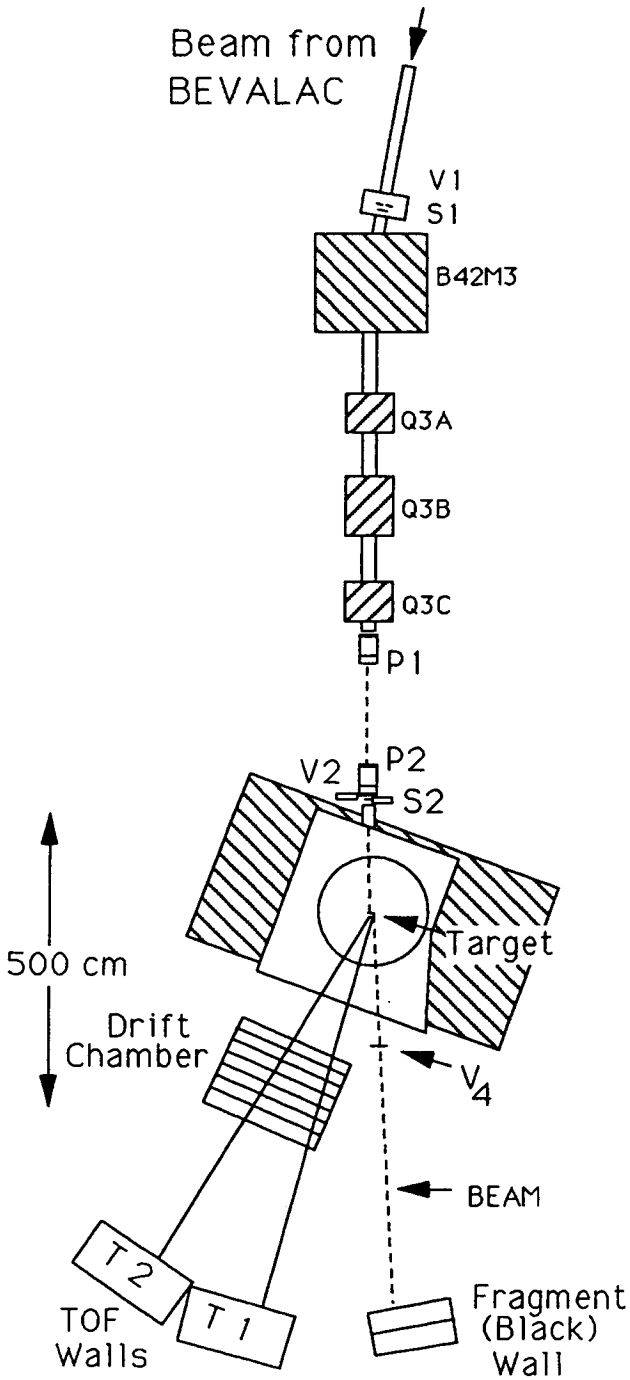
Beam from
BEVALAC
V1
S1
B42M3
Q3A
Q3B
Q3C
P1
V2
P2
S2
Target
500 cm
Drift
Chamber
V4
BEAM
T2
T1
TOF
Walls
Fragment
(Black)
Wall

Figure 1

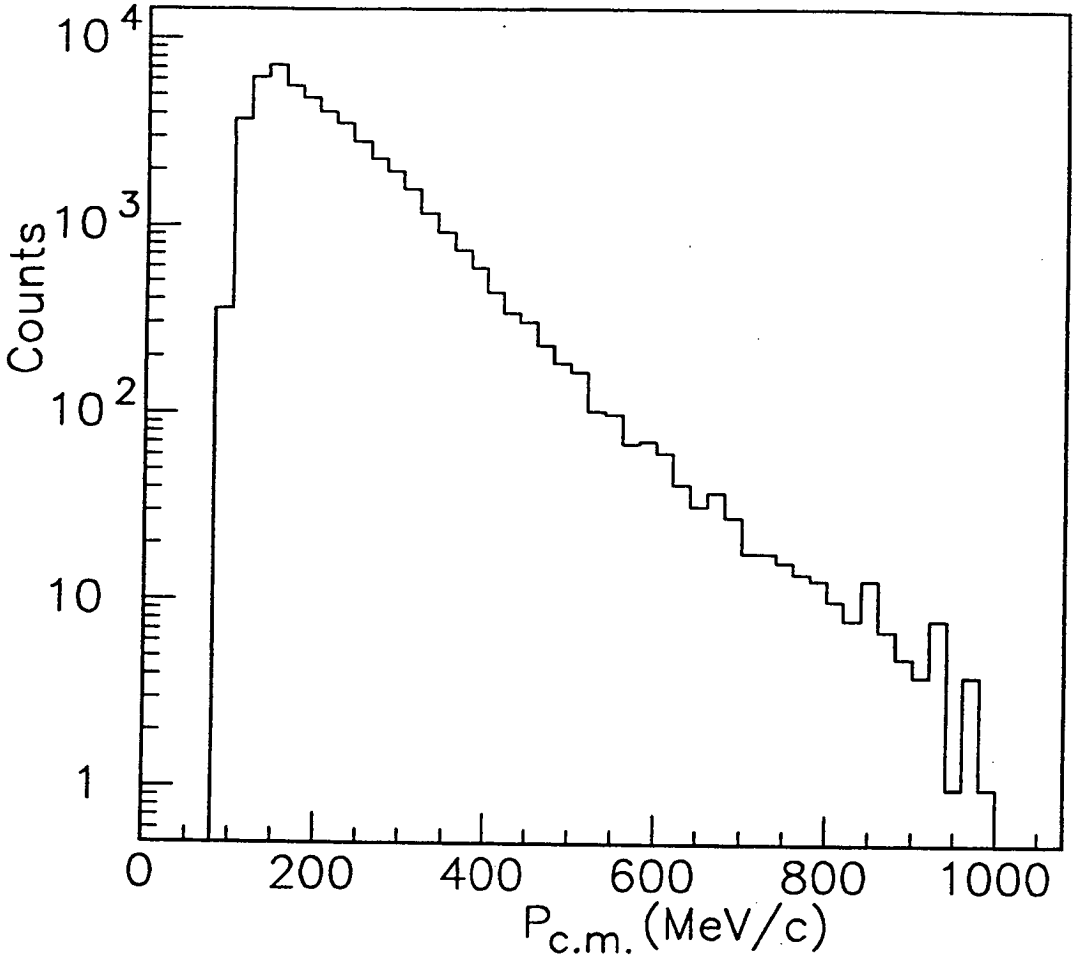

Figure 2

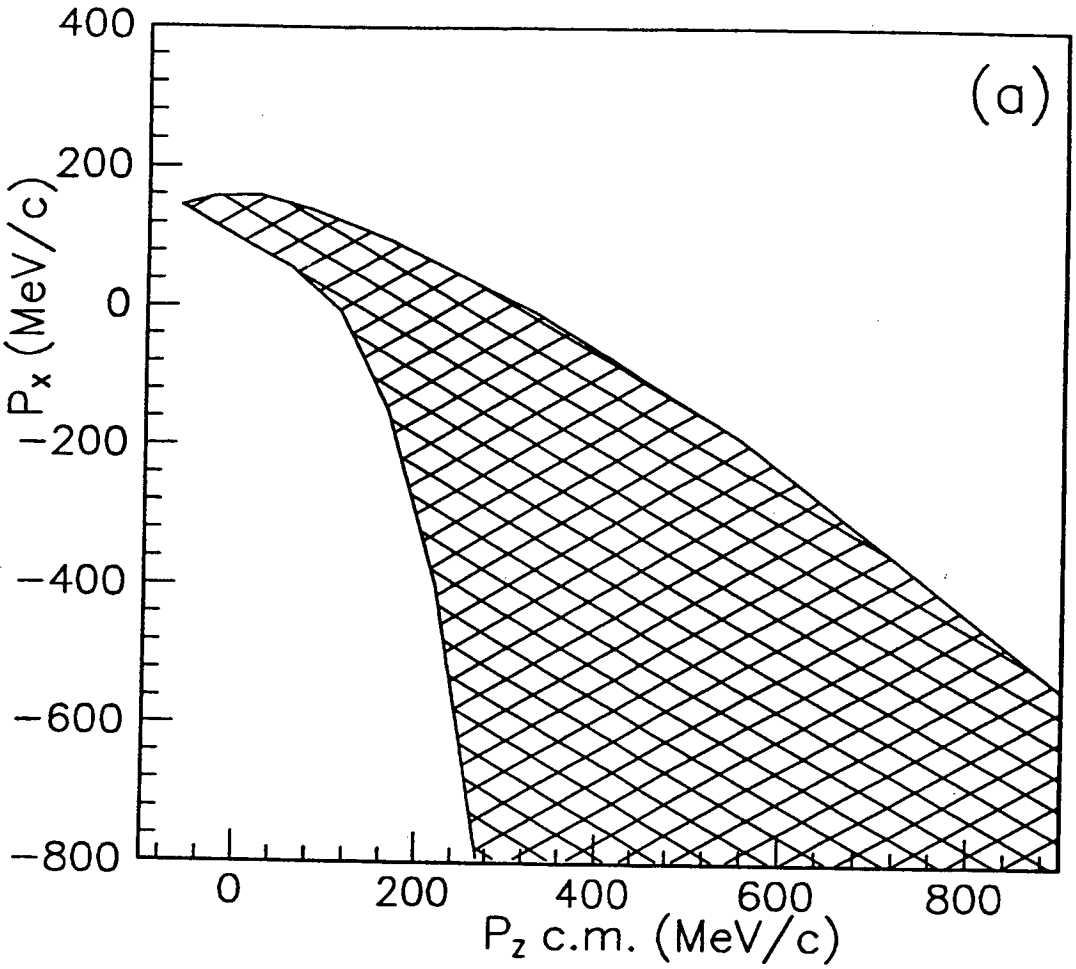

Figure 3 a

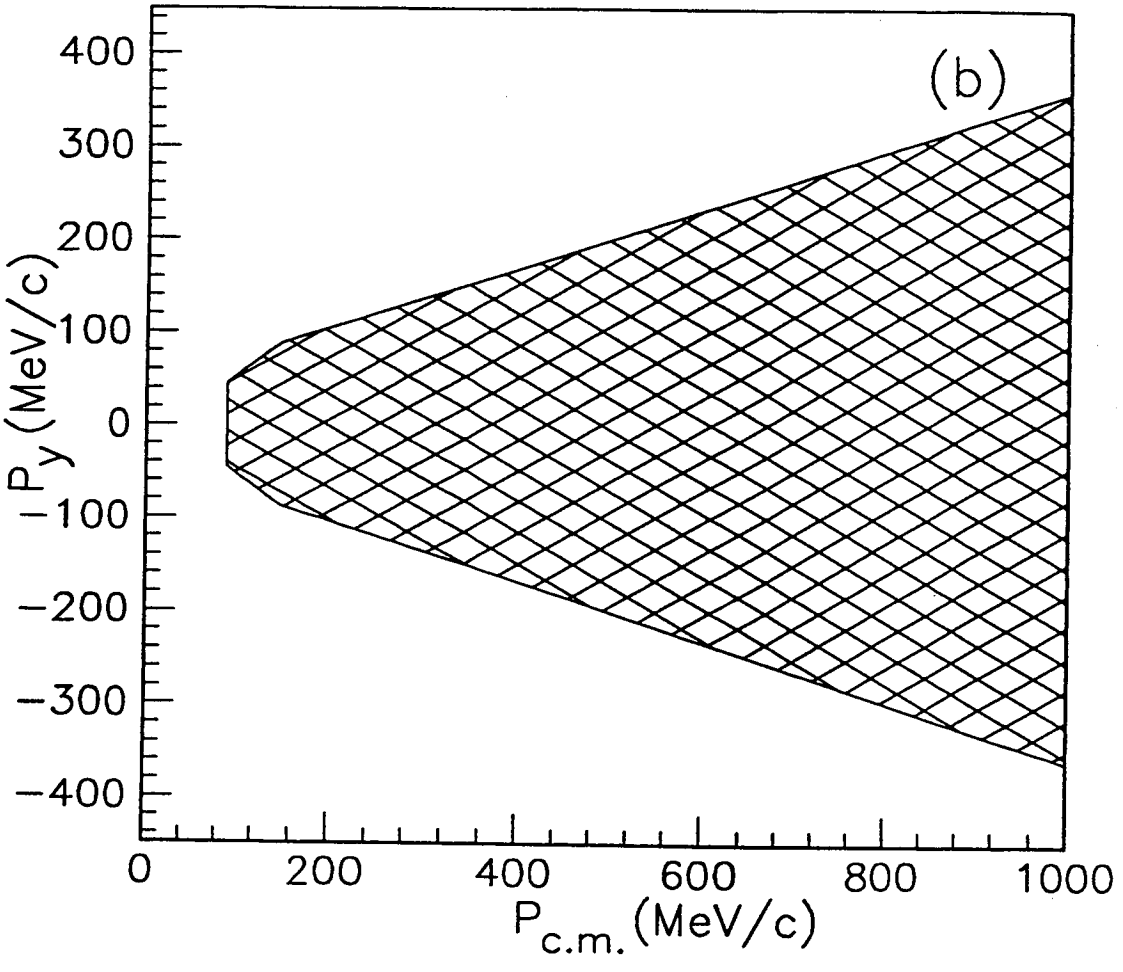
(b)
400
300
200
100
0
−100
−200
−300
−400
P_y (MeV/c)
0
200
400
600
800
1000
$P_{c.m.}$ (MeV/c)

Figure 3 b

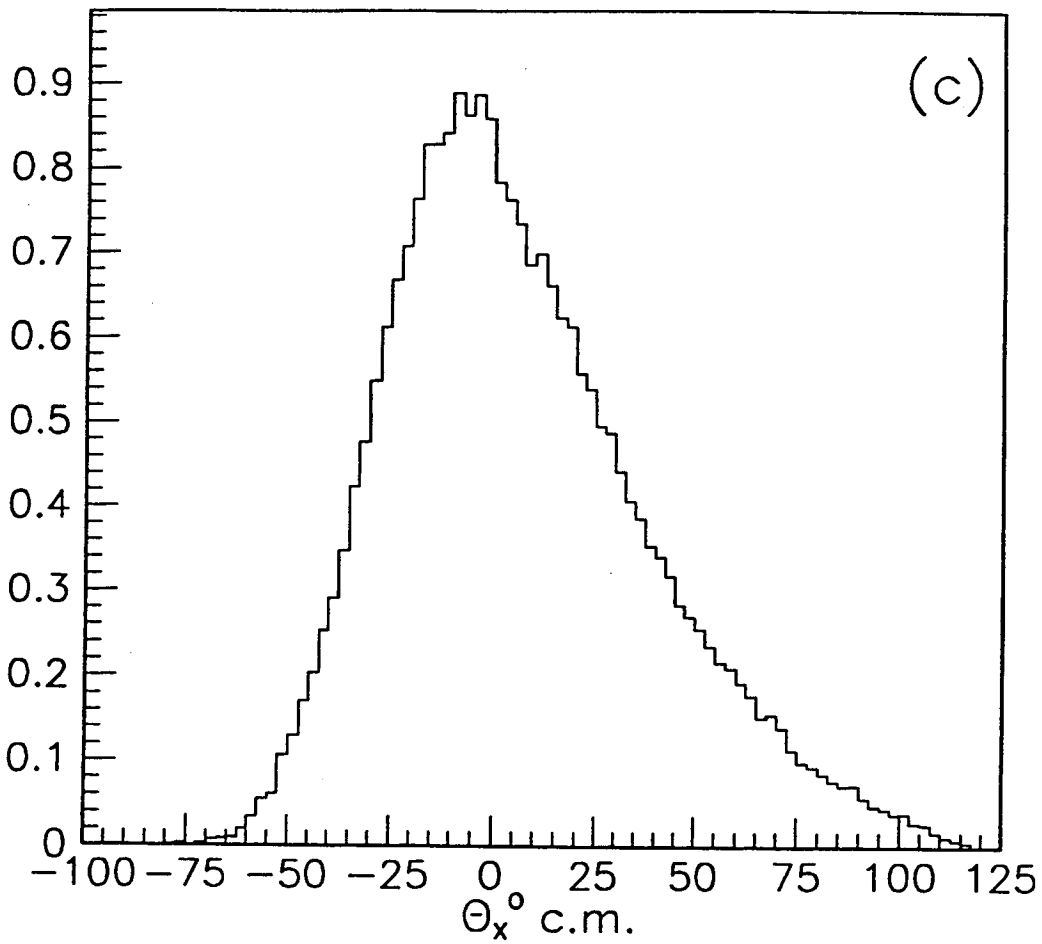

Figure 3 c

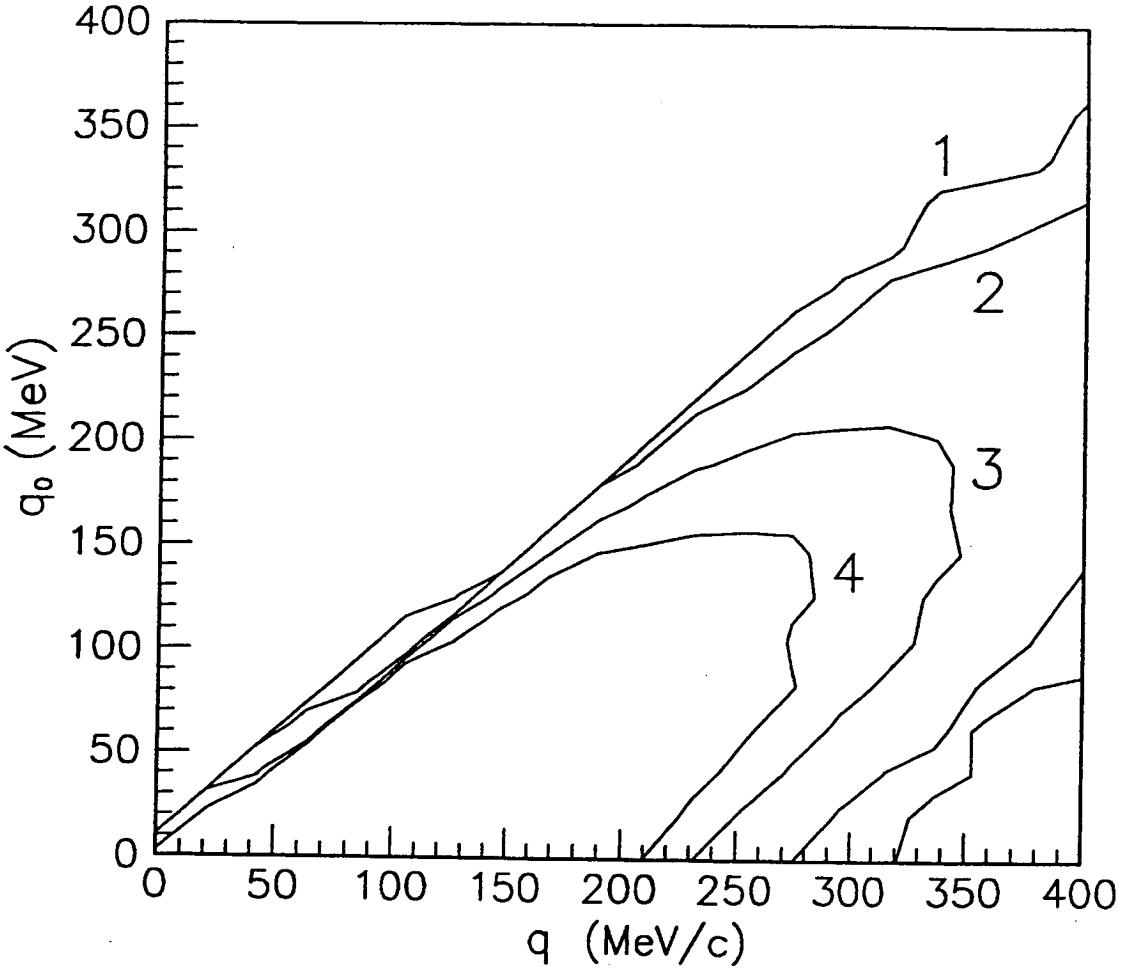
400
350
300
250
200
150
100
50
0
q_0 (MeV)
0
50
100
150
200
250
300
350
400
q (MeV/c)
1
2
3
4

Figure 4

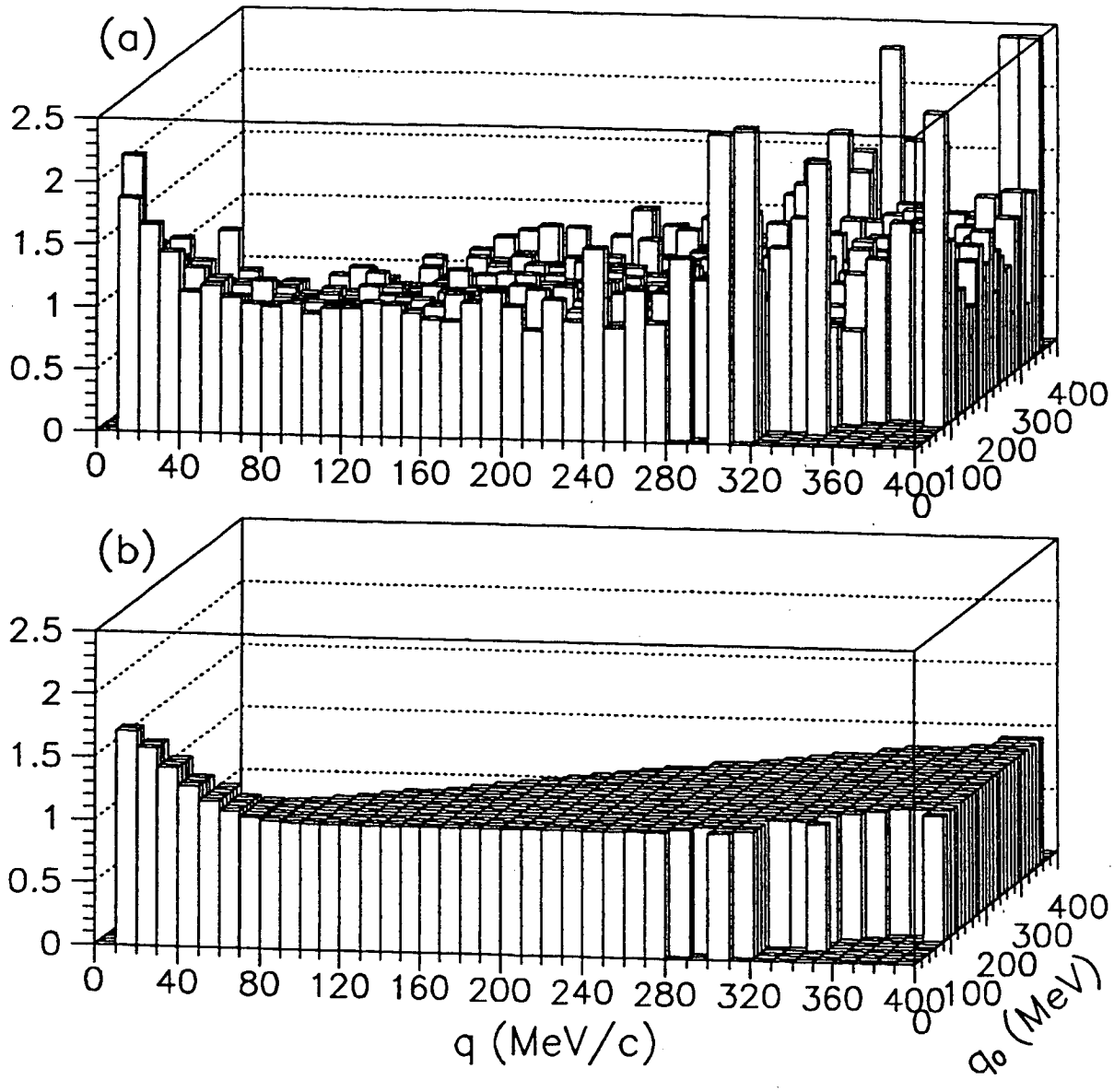
(a)
2.5
2
1.5
1
0.5
0
0 40 80 120 160 200 240 280 320 360 400
0 100 200 300 400
(b)
2.5
2
1.5
1
0.5
0
0 40 80 120 160 200 240 280 320 360 400
q (MeV/c)
0 100 200 300 400
q0 (MeV)

Figure 5

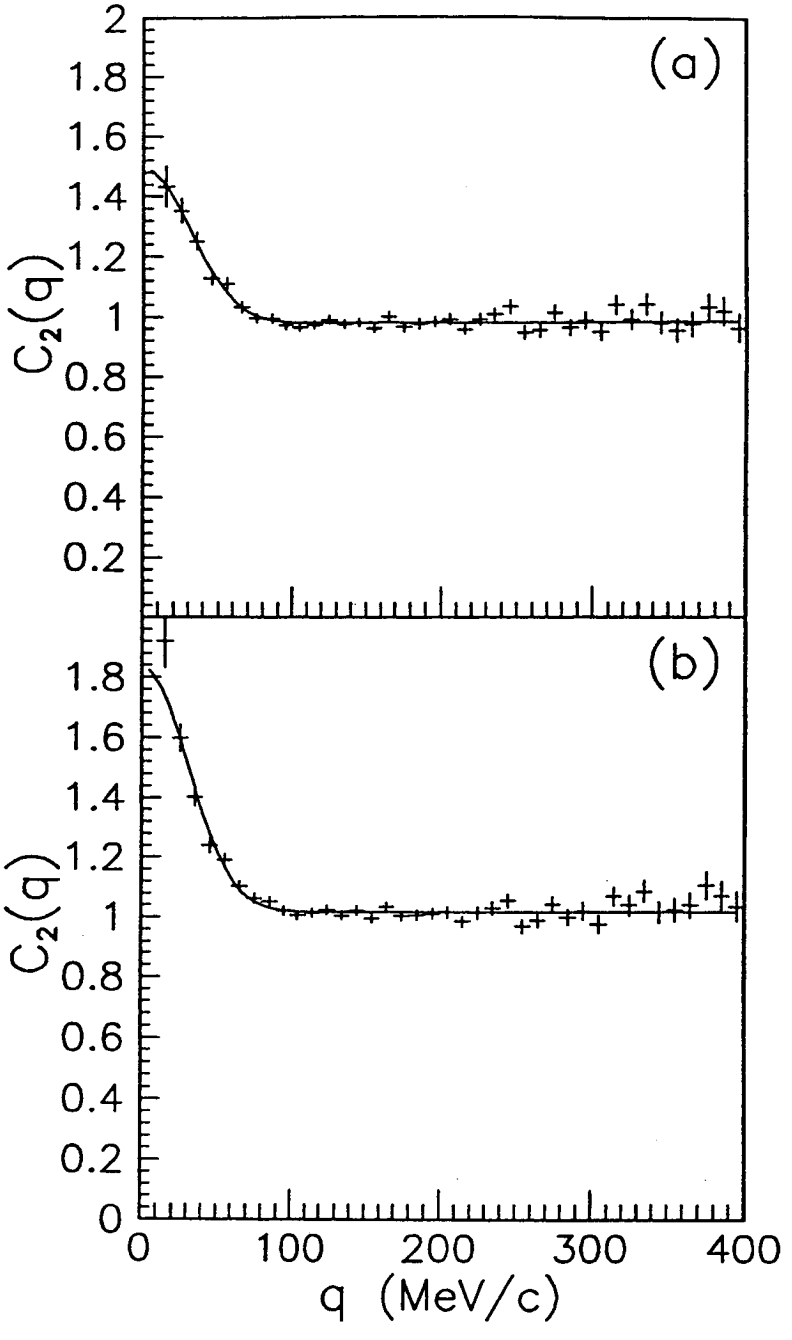

Figure 6

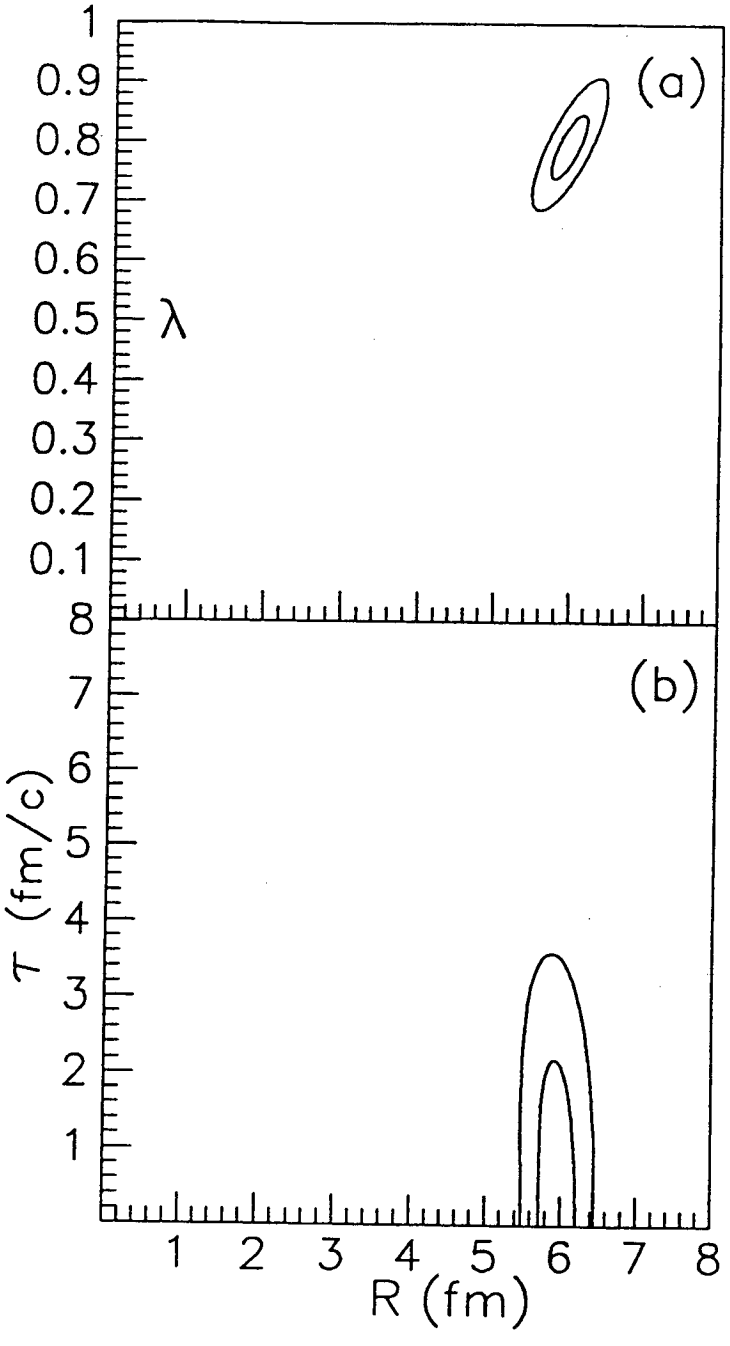

Figure 7

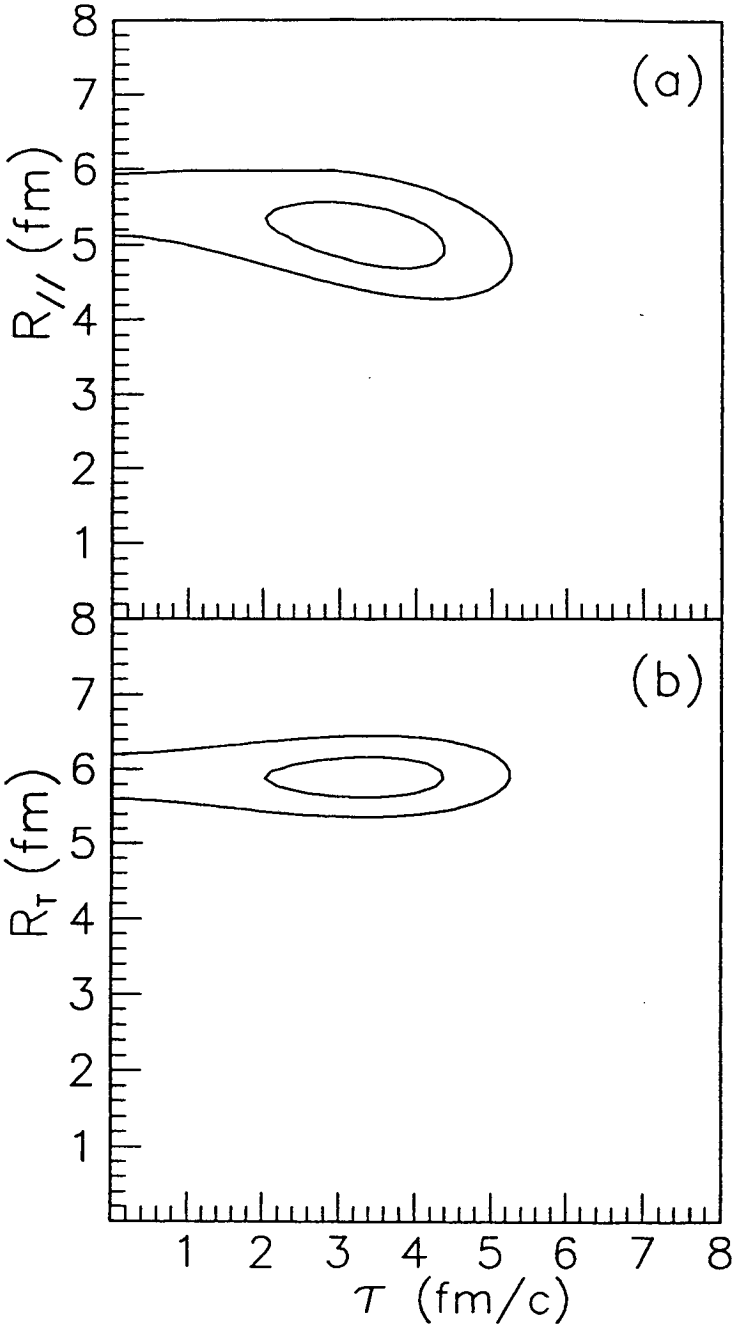

Figure 8

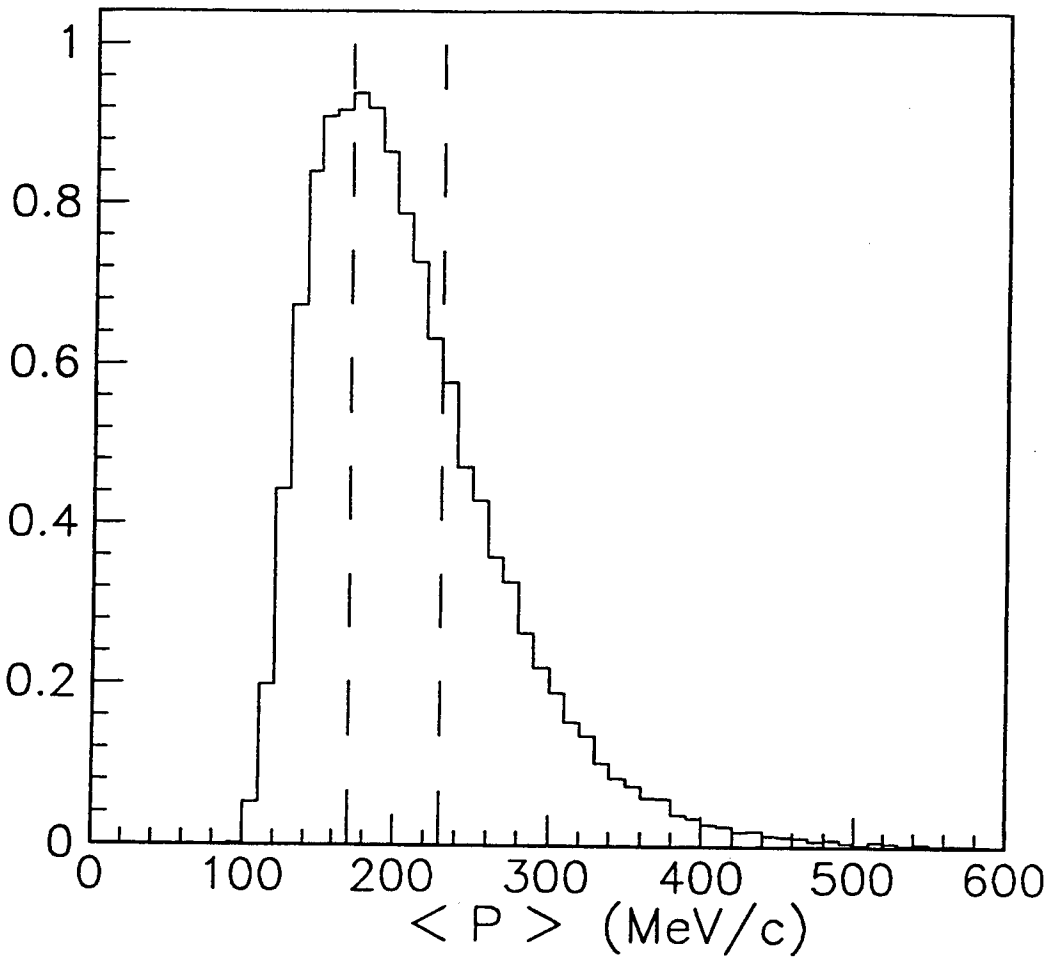

Figure 9

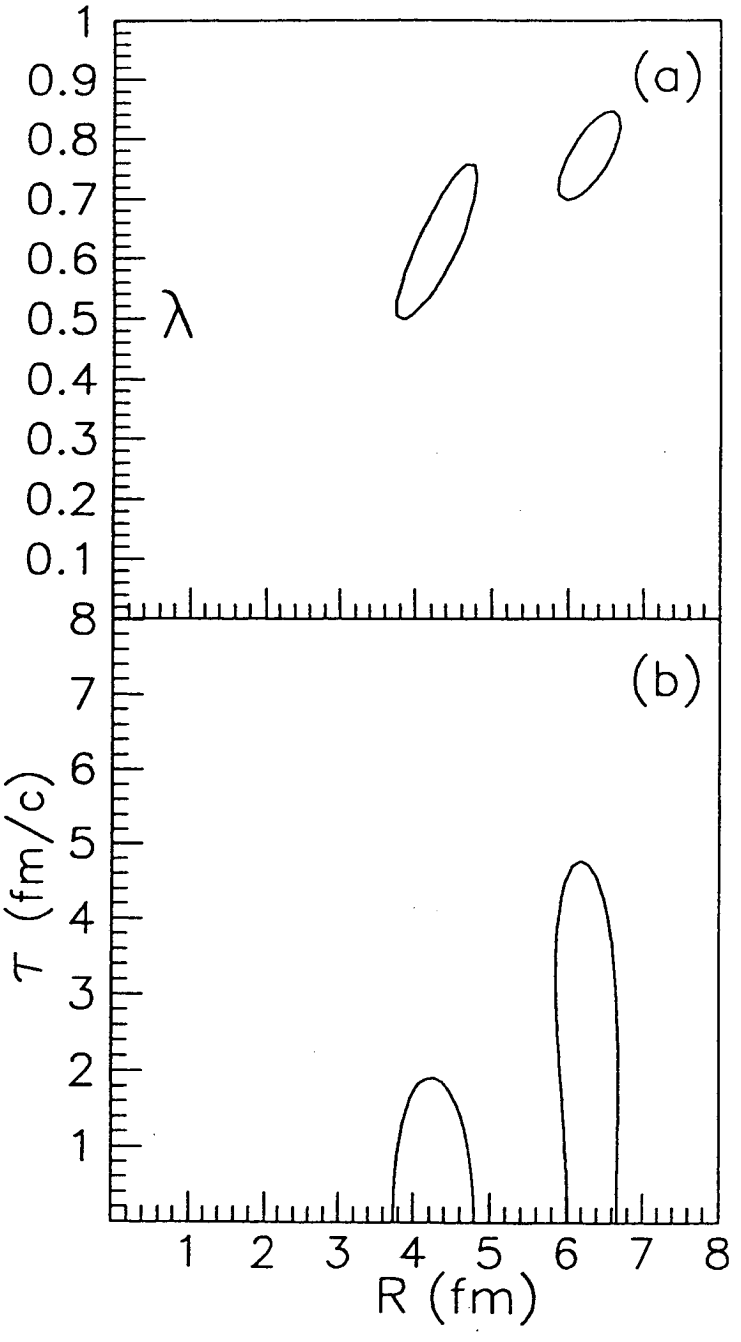

Figure 10

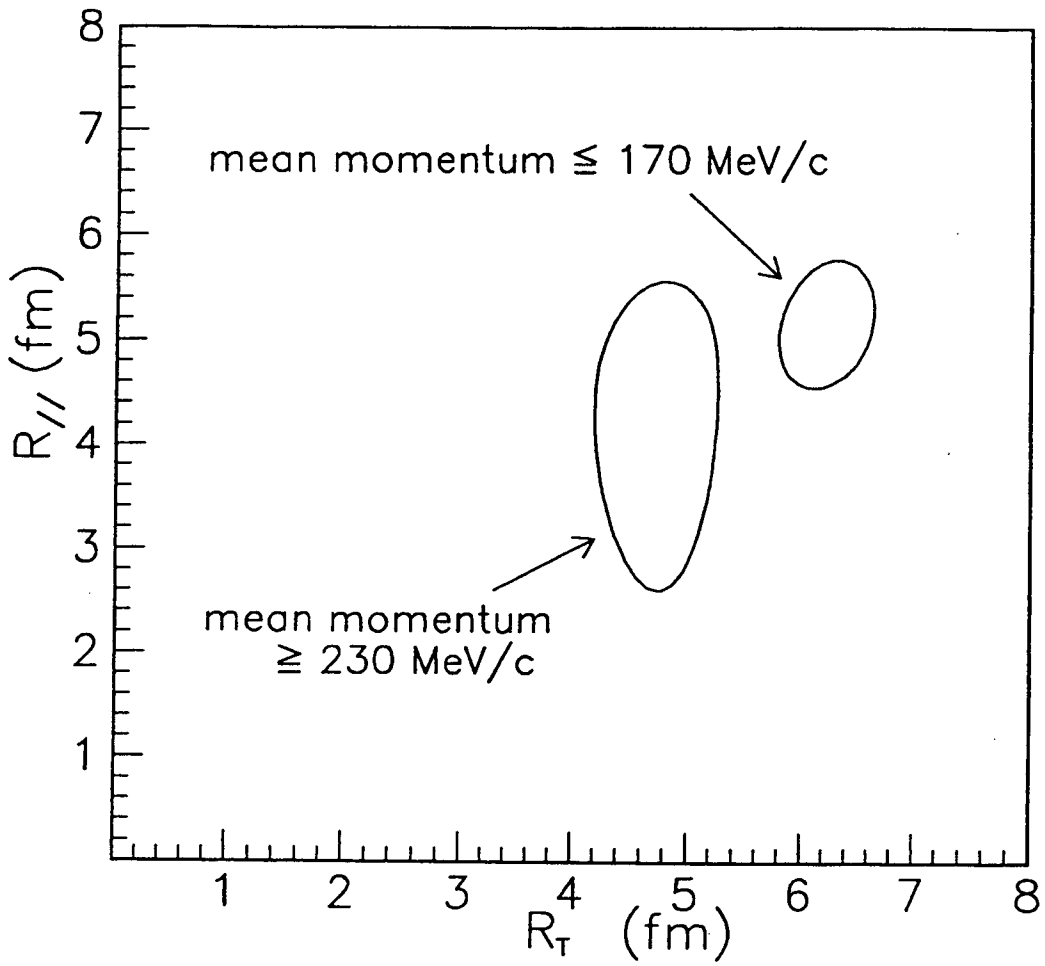
mean momentum ≦ 170 MeV/c
mean momentum
≧ 230 MeV/c
$R_{//}$ (fm)
R_T (fm)
1
2
3
4
5
6
7
8

Figure 11

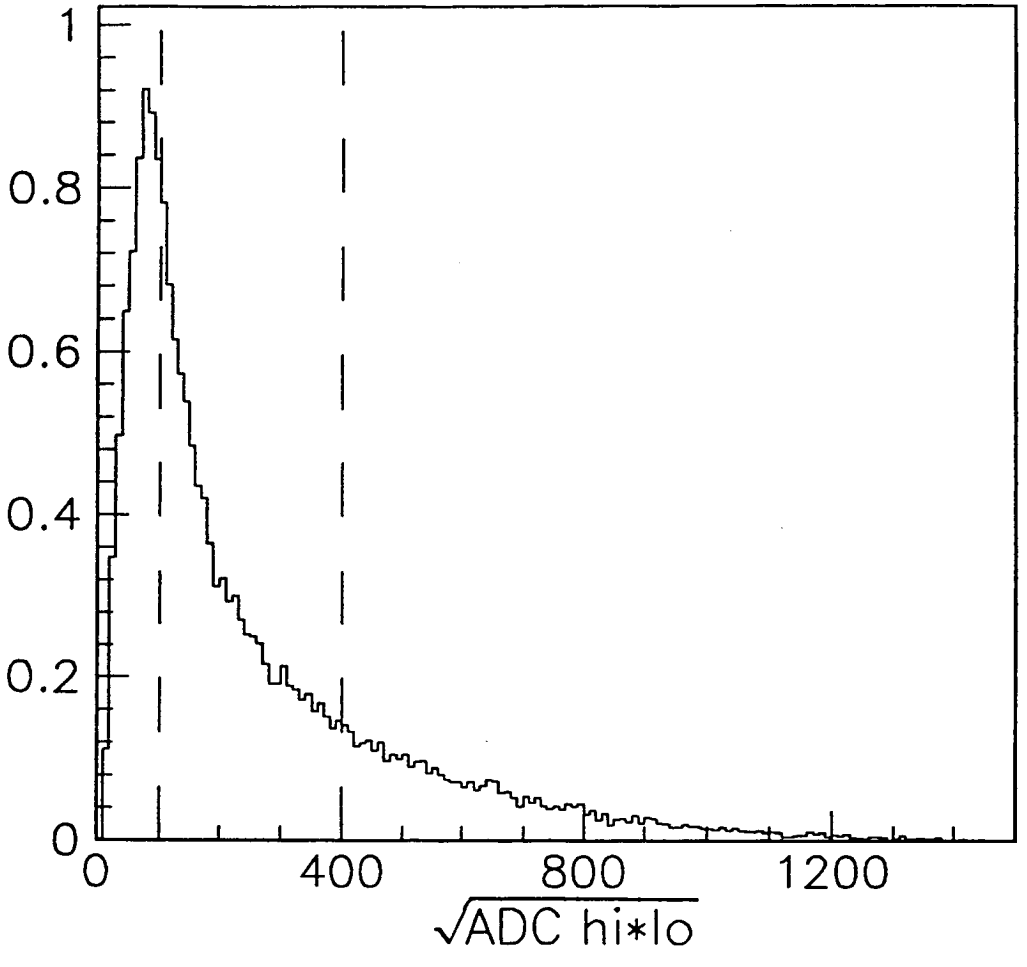

Figure 12

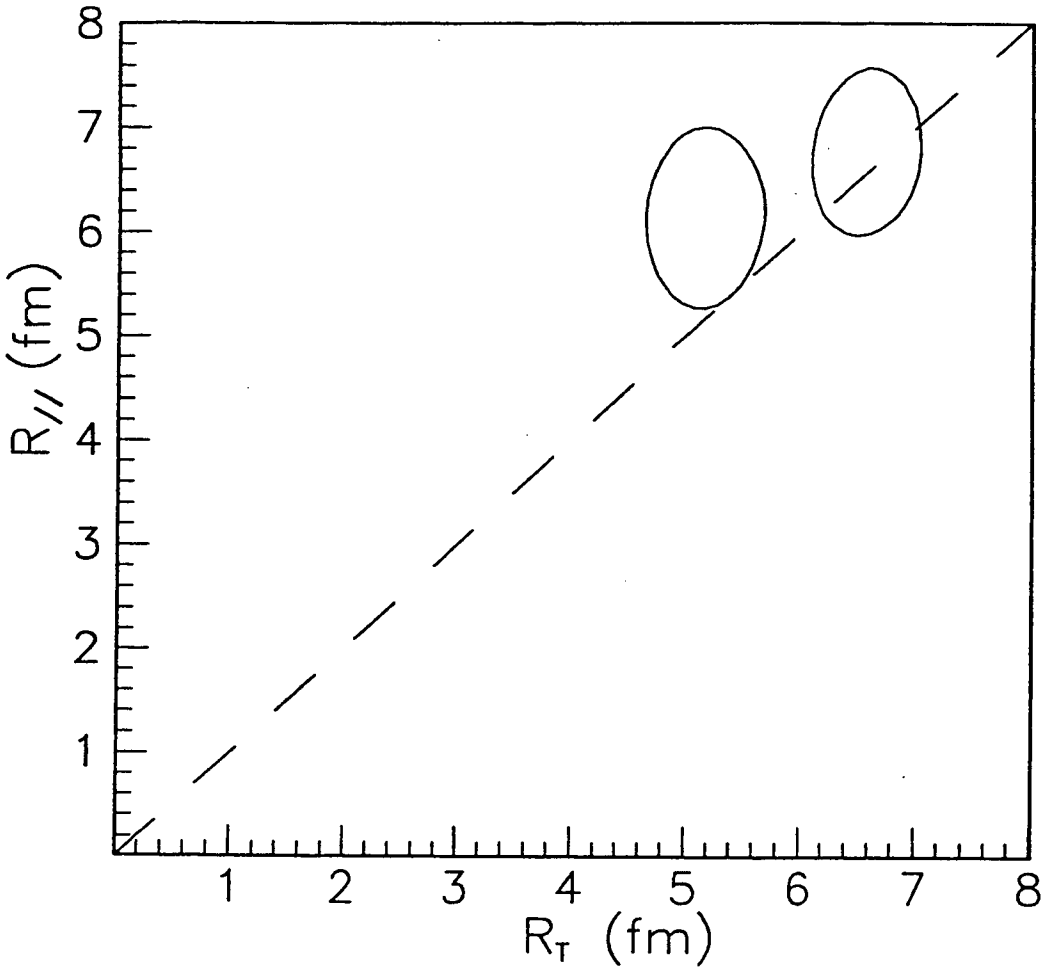

Figure 13

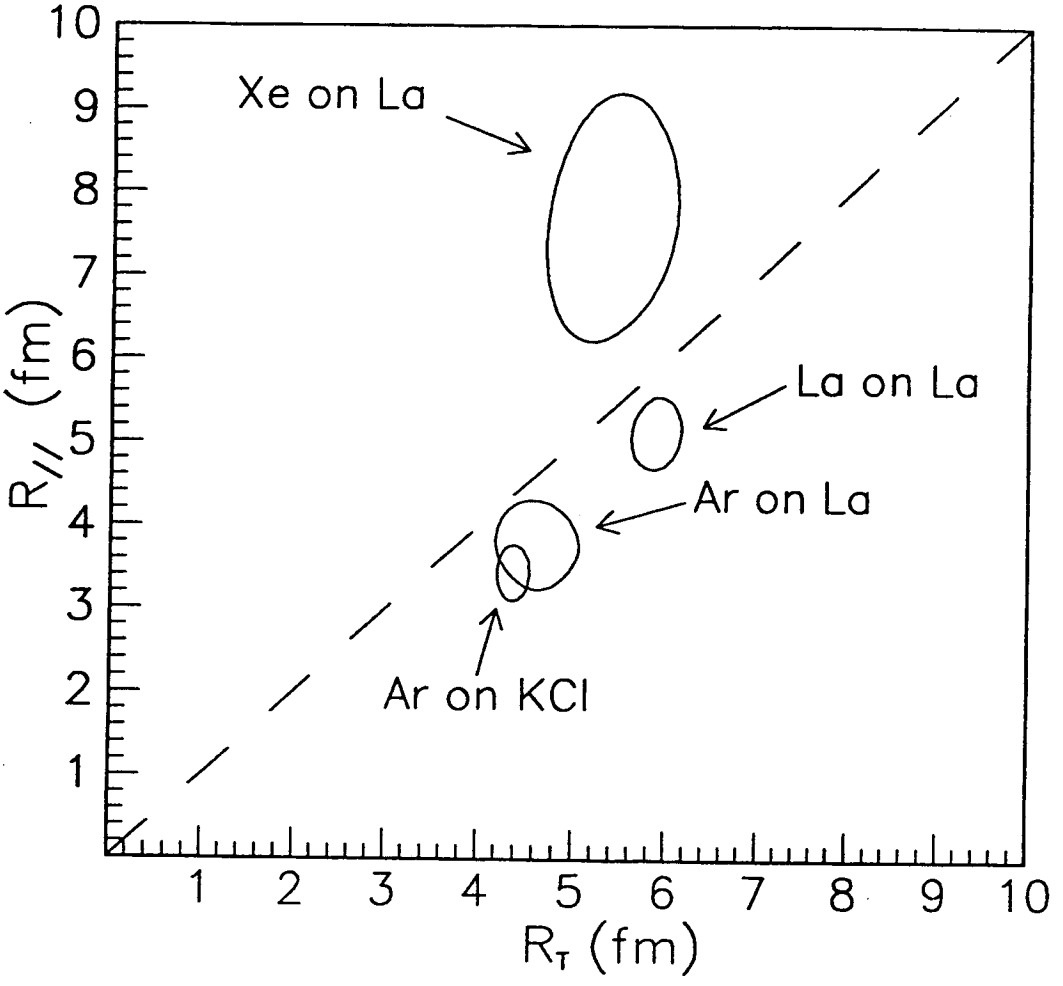

Figure 14

LAWRENCE BERKELEY LABORATORY
UNIVERSITY OF CALIFORNIA
TECHNICAL INFORMATION DEPARTMENT
BERKELEY, CALIFORNIA 94720